Online Resource 1

Supplementary methods and results for Correlated timing errors and terrain dependent uncertainty in synthetic slope microseismic localisation

Journal of Seismology. Lai Wei, Bin Yan, Xiangli Zhang, Yu Chang and Zehao Li. Correspondence: wl20061002@qq.com

Corresponding author affiliation: Department of Electronic Information Engineering, School of Mechanical Engineering and Electronic Information, China University of Geosciences (Wuhan), Wuhan, China

S1 Design and statistical units

Every dataset in this supplement is generated numerically. The timing benchmark uses 200 paired source identities, six surfaces, four receiver counts and four clock scales. At every setting, layered full-covariance and diagonal inversions share observations. Three additional assumptions are tested at 64 receivers. The resulting 52,800 method records are repeated numerical evaluations, not 52,800 independent source events. Structural tests reuse the 200 coordinates with separate noise innovations. Waveform tests use 100 separately generated identities and six conditions per terrain. Calibration events and noise-only threshold records are separated from test data.

Table S1 Fixed numerical parameters

Parameter	Value
Timing generator seed	2026101101
Velocity calibration seed	61001
Timing bootstrap seed	47001
Structural innovation seed	86112
Waveform event seed	2026101102
Waveform noise seeds	810000 + identity
Detector calibration / test negatives	780000 + record / 910000 + record
Interface Z	−15 m
P velocity upper / lower	4000 / 4800 m/s
S velocity upper / lower	2300 / 2800 m/s
P / S independent pick SD	0.12 / 0.18 ms
Inversion starts	[0, 0, −40] m; median(arrivals) −15 ms
Maximum function evaluations	65
Inversion tolerances	ftol = xtol = gtol = 10^{-9}
X/Y bounds	−30 to 30 m
Z bounds	−90 to −15.01 m

Parameter	Value
Origin bounds	150 to 800 ms
Waveform samples / sample rate	4000 / 8000 Hz
Pulse P / S frequencies	310–370 Hz / 0.88 × P
Cross-phase leakage	12%
Bandpass / filter order	120–850 Hz / fourth order
Quiet regression interval	0.025–0.100 s
Detection search interval	0.105–0.445 s
Network smoothing window	129 samples
Pick search half-width	96 samples
Threshold calibration	1.05 × maximum of 80 ordinary negative scores
Pooled figure bootstrap	1000 identity resamples; 500 for detected-event P90

S2 Calibration and solver checks

Table S2 Fitted velocities from 12 independent known sources per terrain

Terrain	P upper	P lower	S upper	S lower
Flat	3997.7	4803.2	2303.0	2798.9
Gentle plane	4005.3	4796.6	2303.1	2798.7
Saddle	4004.1	4797.6	2302.8	2799.0
Steep plane	4009.4	4793.0	2302.4	2799.4
Convex	4002.4	4799.0	2302.3	2799.3
Step	4005.0	4796.5	2301.9	2799.6

Velocities are in m/s. Calibration origins are known and clock perturbations are not injected into calibration records; a 0.03 ms assumed shared covariance is used in fitting. Calibration parameter uncertainty is therefore a local estimate under a favourable controlled-source design. No velocity parameter is fitted to a test hypocentre.

Table S3 Independent implementation checks

Check	Maximum discrepancy
Snell versus Fermat travel time	8.88e-14 ms
Analytic versus finite-difference gradient	4.43e-11 ms/m
Whitened covariance identity	2.22e-15
Noise-free three-start location error	7.42e-13 m
Saved observation reconstruction	1.7e-13 ms
Retained timing boundary / failed solutions	357 / 0

These checks establish consistency of independently implemented numerical routines within the same physical model. They do not establish agreement with observed seismic propagation. The code uses pseudoinversion of the information matrix; no uncertainty ellipsoid is claimed for an unidentifiable or strongly non-linear field case.

S3 Timing results at the principal clock scale

Table S4 P90 errors and conditional coverage at 0.15 ms shared clock deviation

Terrain	N	GLS P90 (m)	Diagonal P90 (m)	GLS coverage (%)	Diagonal coverage (%)
Flat	16	1.130	1.820	95.5	82.0
Flat	64	0.781	2.084	96.5	33.0
Flat	144	0.573	2.091	94.0	15.0
Flat	576	0.332	2.146	91.0	4.0
Gentle plane	16	1.121	1.832	95.5	82.0
Gentle plane	64	0.778	2.065	97.0	34.5
Gentle plane	144	0.555	2.061	93.0	16.0
Gentle plane	576	0.329	2.082	90.5	3.5
Saddle	16	1.124	1.827	95.5	81.5
Saddle	64	0.790	2.058	97.5	34.0
Saddle	144	0.546	2.073	93.0	16.5
Saddle	576	0.327	2.085	90.0	3.5
Steep plane	16	1.145	1.811	95.5	81.0
Steep plane	64	0.819	2.073	96.5	34.0
Steep plane	144	0.557	2.048	94.5	15.5
Steep plane	576	0.331	2.118	90.0	4.0

Terrain	N	GLS P90 (m)	Diagonal P90 (m)	GLS coverage (%)	Diagonal coverage (%)
Convex	16	1.159	1.858	95.5	82.0
Convex	64	0.806	2.120	96.5	34.0
Convex	144	0.585	2.120	93.5	16.0
Convex	576	0.332	2.167	90.5	3.5
Step	16	1.122	1.789	95.5	82.0
Step	64	0.784	2.099	96.5	34.0
Step	144	0.579	2.001	94.5	15.5
Step	576	0.320	2.130	92.0	3.5

Each row uses 200 paired source identities. Full bootstrap intervals and all clock scales are retained in the timing summary CSV in Online Resource 2. A receiver-count comparison holds the outer envelope and timing-group count fixed. Sparse receivers are not a high-frequency alias-free beamforming arrangement.

S4 Structural misspecification

The extra group bias is drawn independently for P and S with 0.15 ms standard deviation. The Gaussian lateral slowness anomaly has centre (5, −3, −30) m and scales (10, 10, 14) m. Its 4% peak amplitude is integrated by 80 equally spaced midpoint samples along a straight segment; the layer velocity used for each sample depends on its elevation. This perturbation is not an exact refracted path through the anomaly. The fitted model remains the calibrated two-layer model, so poor coverage measures misspecification rather than numerical solver disagreement.

The +2% velocity and lateral-anomaly cases are retained even when point-error thresholds appear satisfactory. All phase-bias and anomalous-path records are supplied, including optimisation/boundary flags. Statistical pooling of the six surfaces would not justify a claim about the prevalence of such biases among natural slopes.

S5 Waveform and negative-control results

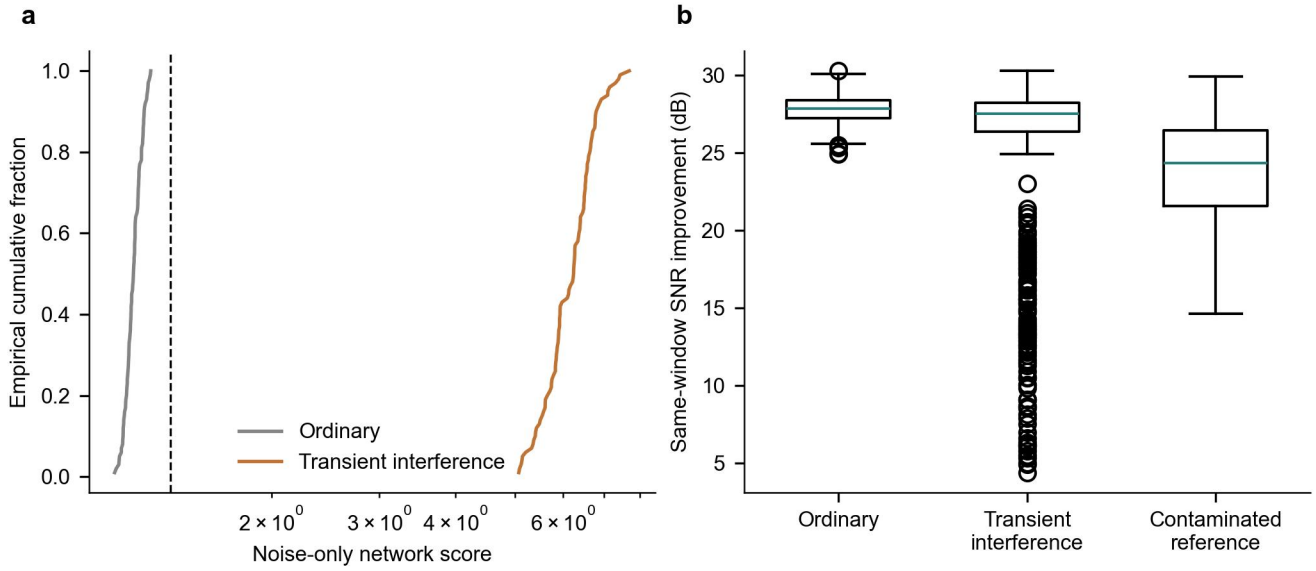


Fig. S1 Negative controls and combined-processing SNR. a Empirical score distributions for 100 held-out records of each noise-only family; the vertical line is the threshold calibrated on 80 separate ordinary negatives. Detection also requires the S peak after the P peak, so score exceedance alone is not the false-positive count. b SNR changes for 600 paired terrain-event records per condition at −6 dB. Boxes show quartiles, median lines and 1.5-IQR whiskers; circles retain outliers. Gains include filtering, reference regression and estimated-delay stacking

Table S5 Held-out noise-only detector outcomes

Noise family	Records	False positives	Fraction
Ordinary	100	0	0.00
Transient interference	100	46	0.46

Negative detection requires both the score threshold and phase-peak ordering. Scores alone do not classify records. Ordinary negatives calibrate the threshold; the transient family is a held-out distributional stress. The score threshold is not adjusted after seeing its 46/100 transient false positives. An observed 0/100 ordinary false-positive count has a Wilson 95% interval of approximately 0–3.7%. The corresponding transient interval is approximately 36.6–55.7%.

Table S6 Waveform stress comparison at −6 dB with 100 identities per condition

Terrain	Condition	Detected n	Detected ≤2 m (%)	Detected P90 (m)
Flat	Ordinary	95	94	0.87
Flat	Transient	96	77	56.41
Flat	Reference leakage	98	5	9.78
Gentle plane	Ordinary	97	96	0.87
Gentle plane	Transient	97	75	61.60
Gentle plane	Reference leakage	100	22	8.82
Saddle	Ordinary	98	95	0.92

Terrain	Condition	Detected n	Detected ≤2 m (%)	Detected P90 (m)
Saddle	Transient	98	74	60.51
Saddle	Reference leakage	100	11	12.54
Steep plane	Ordinary	100	99	1.01
Steep plane	Transient	100	78	63.89
Steep plane	Reference leakage	100	64	5.01
Convex	Ordinary	100	96	0.97
Convex	Transient	100	78	58.40
Convex	Reference leakage	100	12	13.97
Step	Ordinary	98	97	0.96
Step	Transient	99	77	63.28
Step	Reference leakage	99	19	10.21

All three waveform methods and all SNRs are retained in Online Resource 2. Unconditional success treats undetected records as failures; P90 includes every detected source, including large errors. The waveform model is pre-projected, so results do not measure automatic field P/S phase separation. The fixed template outperforming the bank in the controlled pulse family is retained in Fig. 6 and the complete records.

S6 Contextual array pattern calculations

An additional 128-case regular-line calculation uses 24 projected receiver positions, 1.5 m spacing, phase speeds of 2300/4000 m/s, frequencies of 250/500/750/1000 Hz, steering angles of 0/10/20/30 degrees and uniform or 18/25/30 dB Chebyshev weighting. These cuts describe a flat regular array with identical scalar elements. They are contextual pattern calculations, separate from the waveform and two-layer localisation benchmarks.

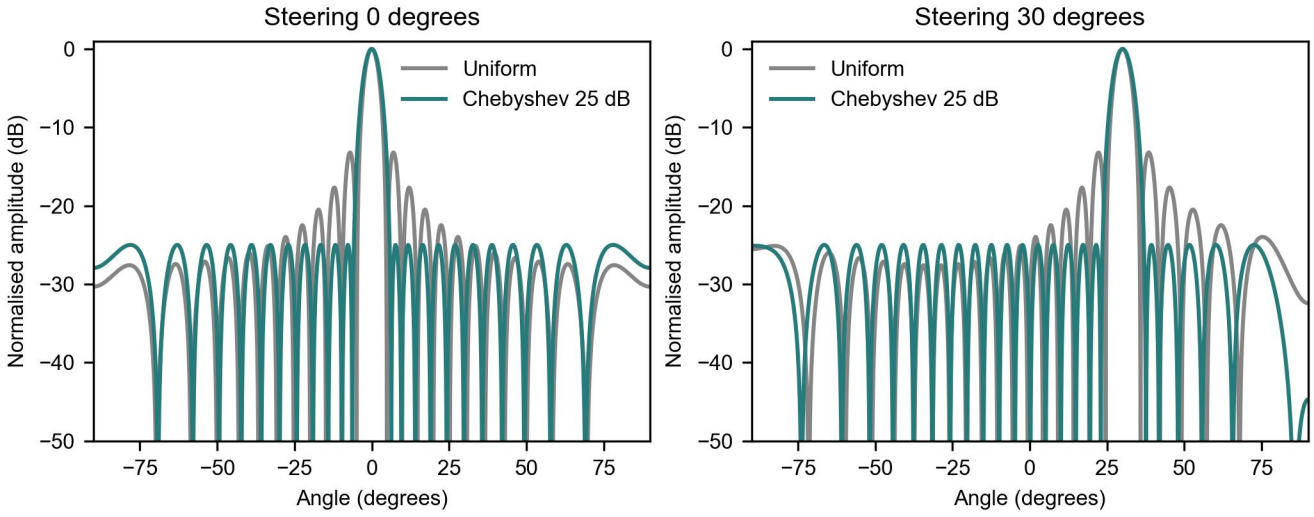


Fig. S2 Contextual far-field angular cuts for a 24-element, 1.5 m projected-spacing line at 750 Hz and 2300 m/s. Steering is 0 and 30 degrees. Uniform and 25 dB Chebyshev weights show the familiar beamwidth–sidelobe trade-off. These flat-plane cuts do not certify full-band, three-dimensional or terrain-dependent alias freedom, and do not measure source-location accuracy

The half-power width is the angular span between the first sampled −3.0103 dB crossings around the commanded main lobe. Cut sidelobe level is the maximum outside its adjacent local minima, retaining any grating lobes. An angle grid of 0.025 degrees is used. Finite-angle truncation and the flat-plane assumption limit interpretation. Low-attenuation Chebyshev windows are used for spatial beam shaping rather than claims about monotonic equivalent spectral noise bandwidth.

A conservative full-visible-space condition for a regular array is $d \leq v/(2f_{max})$. At 2300 m/s and 1.5 m, the associated frequency is 766.7 Hz. At 1000 Hz the S-wave spacing criterion is not met. A limited steering range can have a different bound, but this supplement does not certify a terrain-dependent three-dimensional visible region. The original course-design sweeps are not combined with the new timing identities as extra independent evidence.

S7 Independent calibration repetitions

This extension uses 24 independent calibration-noise batches, each with 12 known sources and 64 calibration receivers. Calibration positions are fixed across batches and terrains; phase noise is independent with P/S standard deviations of 0.12/0.18 ms. Calibration weighting matches these independent variances exactly. Each batch has 30 new test identities with the principal source/depth distributions, giving 720 unique identities paired across terrains, receiver counts and methods. Test clocks have 0.15 ms shared deviation within four groups. Both 64- and 576-receiver arrays are inverted using GLS and diagonal weighting, giving 17,280 location records. Conditional and calibration-propagated ellipsoids use the same GLS point estimate.

The comparison changes calibration noise and test sources together, rather than holding one fitted velocity model fixed. The main calibration experiment deliberately uses a conservative 0.03 ms clock term in the fit, whereas this extension uses the exact independent calibration covariance. It is therefore a separately specified robustness experiment, not a direct replicate of every main-experiment setting. Terrain and receiver-count comparisons within the extension remain paired. Source coordinates, fitted velocities, calibration covariance, all location records and seeds are supplied in Online Resource 2.

Table S7 Joint calibration-and-test coverage with 24 independent batches

Terrain	N	GLS conditional (%)	GLS propagated (%)	Propagated 95% interval (%)	Diagonal (%)
Flat	64	93.5	94.7	92.9–96.4	27.9
Gentle plane	64	93.8	94.7	93.1–96.2	28.3
Saddle	64	93.6	94.7	93.1–96.2	28.5
Steep plane	64	93.8	94.4	92.6–96.1	28.3
Convex	64	93.2	94.6	92.9–96.1	28.2
Step	64	93.2	94.3	92.6–95.8	28.3
Flat	576	84.7	95.0	93.3–96.5	3.1
Gentle plane	576	85.8	95.7	94.0–97.1	3.2
Saddle	576	86.3	95.6	93.8–97.1	3.2
Steep plane	576	86.9	95.4	93.8–96.9	3.8
Convex	576	84.6	94.9	93.2–96.4	3.2
Step	576	84.9	95.1	93.1–96.8	3.3

Coverage intervals use 2000 bootstrap resamples of calibration batches, each retaining 30 test outcomes. The 720 outcomes per row are clustered by calibration fit; pooling as independent Bernoulli trials would omit that dependence. The complete summary also gives conditional and diagonal intervals, P90 errors and optimisation flags. The fixed calibration source geometry, known origin times and correct model family remain favourable conditions.

All 17,280 optimisations are retained, including 0 failed and 0 boundary solutions. This result supports calibration propagation for this model family, not calibrated confidence regions under unknown geology or field waveform errors.

S8 Data and code organisation

Online Resource 2 contains the executable Python scripts, requirements, documentation, CSV trial records, calibration NPZ files and a representative waveform NPZ. File-level SHA-256 hashes identify this release. Receiver coordinates are labelled by terrain, receiver count, receiver index and acquisition group. Timing trial keys are terrain, receiver count, clock scale, method and event identity. Waveform keys are terrain, input SNR, noise mode, method and identity. Calibration origins are known; test origins are estimated.

Stored source inputs and deterministic generators permit waveform records to be regenerated. The package retains full waveform example components but not every multichannel waveform; every test summary and method outcome is stored. Floating-point results may vary slightly across platforms. The implementation-verification script checks the numerical contract without changing the main trial records. No third-party full-text articles are redistributed in the supplementary archive.